parameters GL (pulmonary conductance) and Cdyn (pulmonary compliance) as described[17]. Logarithmically increasing doses of methacholine (3.3–3,300 $\mu g\,kg^{-1}$) were administered intravenously through a jugular venous catheter. Maximally reduced GL and Cdyn values after each methacholine dose were expressed as percentages of their values obtained just before the infusion of that dose. Intervals of 3–5 min were allowed to elaspe between doses to allow GL and Cdyn to return to within 10% of the baseline obtained before the preceding dose.

Segmental allergen challenge of human subjects

Approval for the human study was granted by the Brigham and Women's Hospital Review Board. The study subjects included five control subjects without any history of respiratory disorder, including asthma, and eight allergic asthmatics who met the American Thoracic Society criteria for an asthma diagnosis[27]. Each asthmatic subject had an abnormal allergen skin prick test defined as a weal of greater than 5 mm to 1 of 12 standard allergens in 50% vol/vol glycerin solution (Eastern 10-tree mix, ragweed mix, 3-weed mix, dog epithelium/mixed breeds, timothy grass, *Dermatopagoides farinae*, *D. pteronyssinus Alternaria tenius*, coakroach, *Cladosporium herbarum* and *Aspergillus* mix (all from Greer Laboratories), and cat hair standardized extract (ALK Laboratories)).

Before the study, the subjects were exposed to increasing concentrations of neubulized allergen to determine the concentration required to reduce their FEV_1 by 20%. We performed segmental allergen challenge with seasonal allergens at times when these agents were not in season. At this time all subjects were free of respiratory symptoms and had stable lung function for at least 4 weeks following the inhalation challenge before segmental challenge, for which procedure subjects underwent two serial bronchoscopic procedures 4–8 h apart.

Bronchoscopy was performed under midazolam/fentanyl conscious sedation. For normal and asthmatic pre-allergen samples, the bronchoscope was advanced to airway occlusion in the anterior segment of the left upper lobe and 3 × 50-ml aliquots of warmed sterile saline instilled and gently aspirated; in asthmatics only, the bronchoscope was then moved and advanced into the right upper lobe, where 2 ml of allergen diluent was delivered; after 5 min the bronchoscope was moved again and advanced into the right middle lobe, where 2 ml of allergen solution was delivered. The broncoscope was then removed, and focal wheezing was confirmed to be present exclusively over the right middle lobe in all subjects by auscultation. Four to eight hours later, a second bronchoscopy was performed to obtain BAL fluid from the right upper lobe (sham sample) and the right middle lobe (allergen sample).

Measurement of C3a/C3a des-Arginine levels in BAL fluid

BAL fluid samples were collected onto ice, strained through a gauze mesh and centrifuged (700*g* at 4 °C) and stored at −80 °C until assayed. C3a/C3a des-Arginine levels were measured using an RIA kit (Amersham Pharmacia Biotech). Interference from the precursor C3 in BAL samples was avoided by the inclusion of a selective precipitation step before the assay. All samples were assayed undiluted according to the protocol outlined by the manufacturers.

Received 17 May; accepted 18 July 2000.

1. Burrows, B., Martinez, F. D., Halonen, M., Barbee, R. A. & Cline, M. G. Association of asthma with serum IgE levels and skin-test reactivity to allergens. *N. Engl. J. Med.* **320,** 271–277 (1989).
2. Gerard, N. P. in *Asthma* (eds Barnes, P. J., Grunstein, M. M., Leff, A. R. & Woolcock, A. J.) 639–651 (Lippincott-Raven, Philadelphia, 1997).
3. Medzhitov, R. & Janeway, C. A. Jr. Innate immunity: The virtues of a nonclonal system of recognition. *Cell* **91,** 295–298 (1997).
4. Höpken, U. E., Lu, B., Gerard, N. P. & Gerard, C. The C5a chemoattractant receptor mediates mucosal defence to infection. *Nature* **383,** 86–89 (1996).
5. Höpken, U. E., Lu, B., Gerard, N. P. & Gerard, C. Impaired inflammatory responses in the reverse Arthus Reaction through genetic deletion of the C5a receptor. *J. Exp. Med.* **186,** 749–756 (1997).
6. Osaka, H. *et al.* Expression of C5a receptor in mouse brain: role in signal transduction and neurodegeneration. *Neuroscience* **88,** 1073–1082 (1999).
7. Bhatia, M. Complement factor C5a exerts an anti-inflammatory effect in acute pancreatitis and pancreatitis-associated lung injury. *Am. J. Physiol.* (submitted).
8. Tornetta, M. A., Foley, J. J., Sarau, H. M. & Ames, R. S. The mouse anaphylatoxin C3a receptor. *J. Immunol.* **158,** 5277–5282 (1997).
9. Hsu, M. H. *et al.* Cloning and functional characterization of the mouse C3a anaphylatoxin receptor gene. *Immunogenetics* **47,** 64–72 (1997).
10. Chao, T. H. *et al.* Role of the second extracellular loop of human C3a receptor in agonist binding and receptor function. *J. Biol. Chem.* **274,** 9721–9728 (1999).
11. Fischer, W. H. *et al.* Regulation of the B cell response to T-dependent antigens by classical pathway complement. *J. Immunol.* **157,** 549–556 (1996).
12. Daffern, P. J. *et al.* C3a is a chemotaxin for human eosinophils but not for neutrophils. I. C3a stimulation of neutrophils is secondary to eosinophil activation. *J. Exp. Med.* **181,** 2119–2127 (1995).
13. Nilsson, G. *et al.* C3a and C5a are chemotaxins for human mast cells and act through distinct receptors via a pertussis toxin-sensitive signal transduction pathway. *J. Immunol.* **157,** 1693–1698 (1996).
14. Stimler-Gerard, N. P. & Galli, S. J. Mast cells in anaphylatoxin-induced spasmogenic activity. *J. Immunol.* **138,** 1908–1913 (1987).
15. Stimler, N. P., Gerard, C. & O'Flaherty, J. T. in *Platelet Activating Factor* (eds Benveniste, J & Arnoux, B.) 195–203 (Elsevier, Amsterdam, 1983).
16. Hamelmann, E. *et al.* Noninvasive measurement of airway responsiveness in allergic mice using barometric plethysmography. *Am. J. Respir. Crit. Care Med.* **156,** 766–775 (1992).
17. Martin, T. R., Gerard, N. P., Galli, S. J. & Drazen, J. M. Pulmonary responses to bronchoconstrictor agonists in the mouse. *J. Appl. Physiol.* **64,** 2318–2323 (1988).
18. Smith, J. K., Chi, D. S., Krish, G., Reynolds, S. & Cambron, G. Effect of exercise on complement activity. *Ann. Allergy* **65,** 304–310 (1990).
19. Onodera, H. *et al.* Complement system in status asthmatics: analysis of anti-complementary effects induced by methylprendisolone. *Arerugi* **41,** 1567–1574 (1997).
20. Pepys, J. & Hutchcroft, B. J. Bronchial provocation tests in etiologic diagnosis and analysis of asthma. *Am. J. Respir. Crit. Care Med.* **112,** 829–859 (1975).
21. Bradley, B. L. *et al.* Eosinophils, T-lymphocytes, mast cells, neutrophils and macrophages in bronchial biopsy specimens from atopic subjects with asthma: comparison with biopsy specimens from atopic subjects without asthma and normal control subjects and relationship to bronchial hyperresponsiveness. *J. Allergy Clin. Immunol.* **88,** 661–674 (1991).
22. Drazen, J. M. Asthma therapy with agents preventing leukotriene synthesis or action. *Proc. Assoc. Am. Physicians* **111,** 547–559 (1999).
23. Barnes, P. J. & Belvisi, M. G. in *Asthma* (eds Barnes, P. J., Grunstein, M. M., Leff, A. R. & Woolcock, A. J.) 1051–1063 (Lippincott–Raven, Philadelphia, 1997).
24. Mattoli, S., Soloperto, M., Marini, M. & Fasoli, A. Levels of endothelin in the bronchoalveolar lavage fluid of patients with symptomatic asthma and reversible airflow obstruction. *J. Allergy Clin. Immunol.* **88,** 376–384 (1991).
25. Schwartz, L. B. *et al.* Generation of C3a anaphylatoxin from human C3 by mast cell tryptase. *J. Immunol.* **130,** 1891–1895 (1983).
26. Humbles, A. A. *et al.* Kinetics of eotaxin generation and its relationship to eosinophil accumulation in allergic airways disease: analysis in a guinea pig model *in vivo*. *J. Exp. Med.* **186,** 601–612 (1997).
27. American Thoracic Society. Lung function testing: selection of reference values and interpretative strategies. *Am. Rev. Respir. Dis.* **144,** 1202–1218 (1991).

Acknowledgements

We thank T. Martin and J. Drazen for comments and advice; J. Brewer for assistance; D. Zurakowski for help and advice with analysing the statistics; and the staff of ARCH at Children's Hospital for animal care. This work was supported in part by grants from the NIH to N.P.G. and C.G. at the Perlmutter laboratory and Pfizer Central Research.

Correspondence and requests for materials should be addressed to C.G. (e-mail: gerard_c@gonzo.tch.harvard.edu).

A voltage-dependent channel involved in nutrient uptake by red blood cells infected with the malaria parasite

Sanjay A. Desai*†, Sergey M. Bezrukov‡ & Joshua Zimmerberg†

** The Laboratory of Parasitic Diseases, National Institute of Allergy and Infectious Diseases, ‡ The Laboratory of Physical and Structural Biology, and † The Laboratory of Cellular and Molecular Biophysics, National Institute of Child Health and Development, National Institutes of Health, Bethesda, Maryland 20892, USA*

Growth of the malaria parasite in human red blood cells (RBCs) is accompanied by an increased uptake of many solutes including anions[1], sugars[2], purines[3], amino acids[4] and organic cations[5]. Although the pharmacological properties and selectivity of this uptake suggest that a chloride channel is involved, the precise mechanism has not been identified. Moreover, the location of this uptake in the infected RBC is unknown because tracer studies are complicated by possible uptake through fluid-phase pinocytosis[6] or membranous ducts[7]. Here we have studied the permeability of infected RBCs using the whole-cell voltage-clamp method. With this method, uninfected RBCs had ohmic whole-cell conductances of less than 100 pS, consistent with their low tracer permeabilities[8]. In contrast, trophozoite-infected RBCs exhibited voltage-dependent, non-saturating currents that were 150-fold larger, predominantly carried by anions and abruptly abolished by channel blockers. Patch-clamp measurements and spectral analysis confirmed that a small (< 10 pS) ion channel on the infected RBC surface, present at about 1,000 copies per cell, is responsible for these currents. Because its pharmacological properties and substrate selectivities match those seen with tracer studies, this channel accounts for the increased uptake of small solutes in infected RBCs. The surface location of this new channel

© 2000 Macmillan Magazines Ltd

and its permeability to organic solutes needed for parasite growth indicate that it may have a primary role in a sequential diffusive pathway for parasite nutrient acquisition.

Red blood cells have been difficult to patch clamp because of their small size, high deformability and atypical membrane composition. Whole-cell voltage clamp requires the added complexity of rupturing the small patch of membrane under the pipette, and has not been used to study the permeabilities of human RBCs. We have now obtained whole-cell recordings on these cells by matching the oncotic and hydrostatic forces imposed on the cell when the patch is ruptured with brief electrical pulses (400–600 mV, 0.5–1 ms long). Uninfected human RBCs have small ohmic whole-cell conductances (< 100 pS, $n = 12$ cells; Fig. 1a) in this configuration. We used this method to study ion permeation in single RBCs infected with the human malaria parasite, *Plasmodium falciparum*.

Figure 1b shows the whole-cell current in response to voltage steps applied to a trophozoite-infected RBC. This current is 150-fold larger than that of uninfected RBCs ($n = 13$ infected cells; $P < 0.0001$). It exhibited inward rectification (the plateau at positive voltages; Fig. 1c, filled circles) despite using identical solutions on both sides of the RBC membrane, indicating either voltage-dependent gating or rectification of one or more transport pathways in the membrane. We found that the currents could be abruptly abolished by addition of 125 μM furosemide to the bath solution (Fig. 1c, open circles). Furthermore, these whole-cell currents did not saturate at up to 1.1 M salt solutions (Fig. 1d). These findings suggest a single pathway with channel-type transport on the infected RBC membrane.

To examine the ion selectivity of this pathway, we applied a NaCl gradient across the RBC membrane (Fig. 1e). The reversal potential, E_{rev}, under these conditions shifted to −47 mV (mean of 5 cells), approximating the Nernst potential for Cl^- in this experiment (−49 mV measured with a Cl^- electrode). This E_{rev} indicates a strong selectivity for Cl^- over Na^+ and is consistent with tracer studies. (We calculate a Na^+ to Cl^- permeability ratio, P_{Na}/P_{Cl}, of roughly 10^{-5} from the data in refs 1 and 9.)

The pharmacological properties of this conductive pathway are also consistent with previous tracer studies: furosemide, NPPB (5-nitro-2-(3-phenylpropylamino)benzoic acid), niflumate[1], glybenclamide[10] and phloridzin[11] reduced the whole-cell current in low micromolar concentrations, whereas DIDS[12] (4,4′-diisothiocyanatostibene-2,2′-disulphonic acid) had only a modest effect (Table 1). Interestingly, phloridzin had a greater blocking effect in the pipette solution than in the bath, implicating an intracellular site of action as previously proposed[11].

Permeability ratios (P/P_{Cl}) for other anions, determined by E_{rev} measurements, indicate weak selectivity of this pathway, with high permeation rates for large organic anions (Table 2). We found a permeability sequence of $SCN^- > I^- > Br^- > Cl^- >$ acetate$^-$ > lactate$^-$ > glutamate$^-$, corresponding to the Eisenman selectivity sequence number 1 for anions. This suggests permeation through a pathway that has a weak binding site with a large radius[13]; it is inconsistent with a rigid non-interacting pore. (Using data in refs 1, 2 and 9, we calculated P/P_{Cl} for lactate and glutamate to be about 0.5 and 0.03, respectively, which are comparable with our measurements.)

This whole-cell current on infected cells requires transmembrane movement of anions from the bath solution into RBC cytosol. This might occur directly through the exposed RBC plasma membrane. Alternatively, anions might bypass the RBC membrane by moving down the proposed parasitophorous duct (a membranous tubule that may provide the parasite access to serum[7]), and then enter the RBC cytosol through known channels[14] on the parasitophorous vacuolar membrane (PVM), which surrounds the parasite.

To distinguish between surface and duct-associated sites, we used the on-cell patch-clamp method to measure directly transport across patches of RBC plasma membrane. Membrane patches on infected cells often showed a rectifying current (Fig. 2a), suggesting a small conductance ion channel on the infected RBC surface. Prompted by these findings, we used a solution with a high Cl^- concentration (1.15 M) in the bath and pipette to increase conductance. This maneouvre revealed unambiguous channel activity with fast gating and a slope conductance of 20 pS (Fig. 2b, c), suggesting permeation through a proteineous pore rather than a nonspecific membrane defect[15]. This channel exhibited voltage-dependent gating which explains the inward rectification seen with whole-cell measurements (Fig. 2d). It was present in high density on trophozoite-infected cells (37 of 46 patches, 19 with > 3 channels), never on uninfected red cells (22 patches) and could be blocked with 200 μM furosemide in the pipette (much reduced channel activity, $n = 4$ patches on 4 infected cells; Fig. 2e).

This small channel exhibits complex gating with bursts of fast flickering open events and long intervening closed periods (Fig. 2c). Consistent with this complex gating, the spectral density of an on-cell recording revealed a $1/f$ profile[16] (Fig. 3, bottom curve). (A channel with simple, non-bursting gating would have a Lorenztian

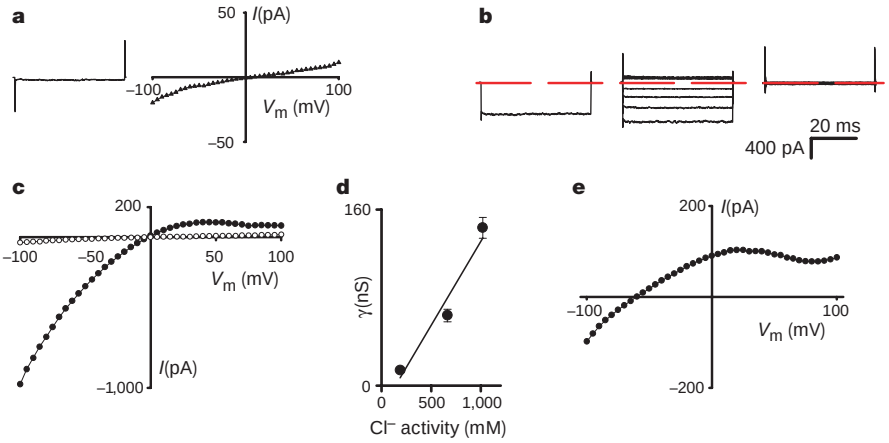

Figure 1 Whole-cell recordings. **a**, Uninfected RBC in solution A. Left, whole-cell current response to a −70 mV pulse. Note the small current amplitude and the capacitive spikes, which reflect patch rupture. Right, corresponding $I-V$ plot. **b**, Trophozoite-infected RBC. Left, recorded as in **a**. Current is 150 times larger than that on uninfected RBCs. Middle and right, responses to pulses of −80 to +80 mV (20-mV increments) before and after bath addition of 125 μM furosemide, respectively. Dashed line represents zero current. **c**, Corresponding $I-V$ plots before (filled circles) and after (open circles) addition of furosemide. **d**, Whole-cell chord conductances in solution A plus 0, 500 or 1,000 mM choline$^+$Cl$^-$. Chord conductances, determined between −50 and −80 mV , are plotted against Cl^- activity (mean ± s.e.m. of 12, 7 and 8 cells, respectively). **e**, Whole-cell $I-V$ plot with solution A in the bath and solution B in the pipette. The negative E_{rev} (or x intercept) confirms a predominance of Cl^- permeation.

© 2000 Macmillan Magazines Ltd

spectral density.) Spectral analysis of our whole-cell recordings also revealed a $1/f$ profile in 140 mM and 1.15 M Cl^- solutions (Fig. 3, middle and top curves, respectively). These parallel profiles, combined with its voltage-dependent gating and the effects of furosemide (Fig. 2d, e), strongly suggest that the small surface channel is the predominant conductive pathway in the infected RBC membrane. Because the spectra of individual channels add up to the whole-cell spectrum, this method also provides an accurate estimate of the channel's functional copy number on this trophozoite-infected cell at about 1,000 (calculated from the single-channel and whole-cell spectra with 1.15 M Cl^-). Calculations using our single-channel and whole-cell conductances, although less precise than spectral methods, indicate that the functional copy number may rise to about 8,000 per cell depending on parasite maturity.

Because its pharmacology and selectivity match those identified by more than 20 years of tracer flux and osmotic lysis experiments[1–5,9–12], this voltage-dependent channel fully accounts for the increased uptake of small solutes into infected RBCs by the "new permeation pathways". Tracer studies have revealed that this channel is permeable to sugars[2], purines[3], amino acids[4] and some organic cations such as choline[5], all of which are required for parasite growth[17]. By localizing this channel to the RBC plasma membrane, our findings indicate that it may have a role in acquisition of these nutrients from serum. Our model is a sequential diffusive pathway for nutrient uptake by the parasite (Fig. 4). Small nutrient solutes in serum can enter the RBC cytosol through this channel. (Whereas most nutrients enter predominantly through this channel, sugars enter primarily through the RBC's endogenous carriers[18].) They would then diffuse through the RBC cytosol and cross the PVM through non-selective 150 pS channels[14] (which show different gating from the surface channel) into the vacuolar space. Finally, they would be taken up by the parasite by specific carriers, some recently identified[19]. Our identified channel is probably also involved in metabolic waste removal (such as lactate, Table 2) and volume regulation of infected RBCs[1]. Its small single-channel conductance and strong selectivity against Na^+, despite permeability to bulky uncharged and charged metabolites, pose intriguing pore-design problems, which may be partly solved by its weak binding site (Eisenman selectivity sequence number 1 for anions) and its voltage-dependence.

With all the steps for this sequential nutrient acquisition pathway identified, the need for a parasitophorous duct to provide a parallel route for uptake of serum nutrients becomes less clear. Moreover, the parasitophorous duct—a proposal based on fluorescent macromolecule uptake by infected cells—remains controversial because

Table 1 Pharmacological properties of the whole-cell currents

Channel blocker	% inhibition
Furosemide	
1 μM (5)	30 ± 12
15 μM (5)	54 ± 9
100 μM (11)	83 ± 2
Glybenclamide	
100 μM (5)	85 ± 9
Niflumate	
2 μM (3)	20 ± 9
18 μM (3)	56 ± 8
78 μM (2)	87
NPPB	
0.8 μM (5)	41 ± 5
8 μM (4)	78 ± 8
32 μM (4)	92 ± 2
DIDS	
100 μM (2)	7
Phloridzin	
300 μM (2)	34
50 μM pipette (3)*	75 ± 2

The percentage inhibition (mean ± s.e.m.) of whole-cell currents on bath addition of channel blockers at indicated concentrations.
* Phloridzin was also tested by addition to the pipette and chord conductance measurement as in Fig. 1d.

Table 2 Anion selectivity properties of the whole-cell currents

Anion		E_{rev}	P/P_{Cl}
SCN^-	(5)	+50 ± 3	7.4
I^- in bath	(4)*	–31 ± 5	3.5
Br^-	(4)	+4 ± 1	1.2
$Acetate^-$	(3)	–4 ± 1	0.87
$Lactate^-$	(4)	–24 ± 6	0.43
$Glutamate^-$	(5)	–51 ± 3	0.11

The permeabilities of test anions relative to that of Cl^-.
* Iodide was tested by switching the bath and pipette solutions and using an agar bridge. NaS_2O_3 (1.1 mM) was added to the NaI solution as an antioxidant. The number of cells tested at each concentration is given in parentheses.

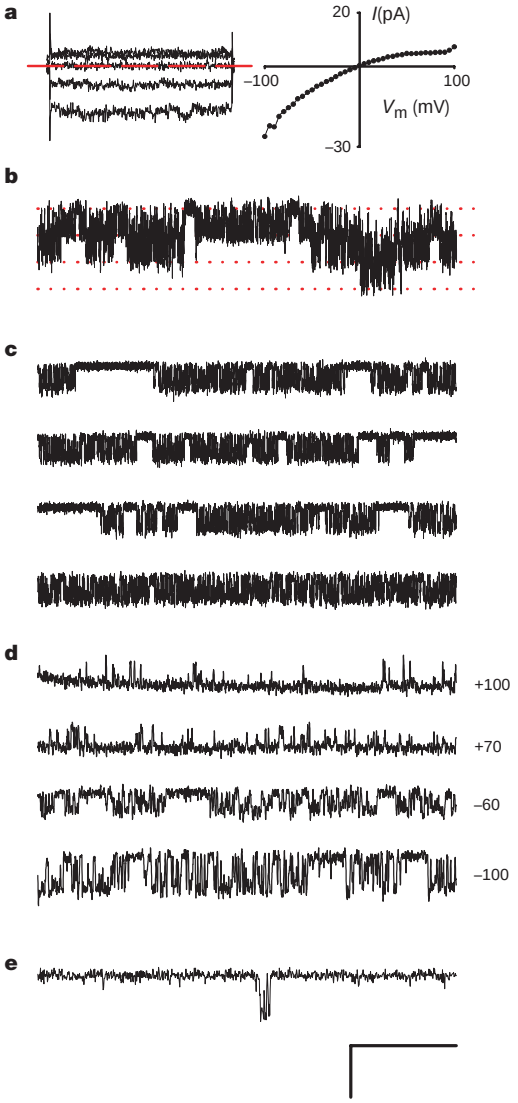

Figure 2 On-cell currents on trophozoite-infected RBCs. **a**, Left, currents in solution A. V_m (membrane potential, negative of pipette potential) pulses were from –80 to +80 mV (40-mV increments). Dashed line represents zero current. This patch had several small channels. Right, corresponding $I-V$ plot. **b**, Currents in solution A plus 1,000 mM choline$^+Cl^-$. This on-cell patch had three independent and identical channels, whose opening events are represented by downward deflections. V_m, –100 mV . **c**, A single-channel patch showing fast flickering and complex burst behaviour. Seal resistance was 150 GΩ. **d**, Voltage-dependent gating at indicated V_m (millivolts). The channel opens more frequently at negative V_m (downward deflections) than at positive V_m (upward deflections). **e**, Identical conductance but fewer opening events with 200 μM furosemide in the pipette. V_m ,–100 mV (Compare the bottom trace in **d**, without furosemide.) Scale bars, 19.5 pA/29 ms (**a**); 4.4 pA/71 ms (**b**); 4.4 pA/48 ms (**c**); 3 pA/12 ms (**d**, **e**).

© 2000 Macmillan Magazines Ltd

of poor reproducibility[20] and an absence of definitive electron microscopic evidence. If the duct exists, it should produce a furosemide-insensitive current in our whole-cell measurements that involves diffusion down the duct, into the vacuolar space around the parasite and through the PVM channels[14] to the recording pipette. We could not distinguish the currents on furosemide-treated infected cells from those of uninfected cells, implying no electrical continuity between the bath and the vacuole around the parasite. Other models for the proposed duct, such as an intermittently present duct or compartmentalization of the vacuolar space with tight junctions, cannot be excluded with our measurements.

This voltage-dependent channel, found only on infected RBCs, may be either a modified host RBC protein[21] or a parasite-encoded protein targeted to the host membrane[22]. In either case, its exposed location on infected cells and presence in all studied plasmodial species[23] suggest that it may be an ideal target for future chemotherapy development. □

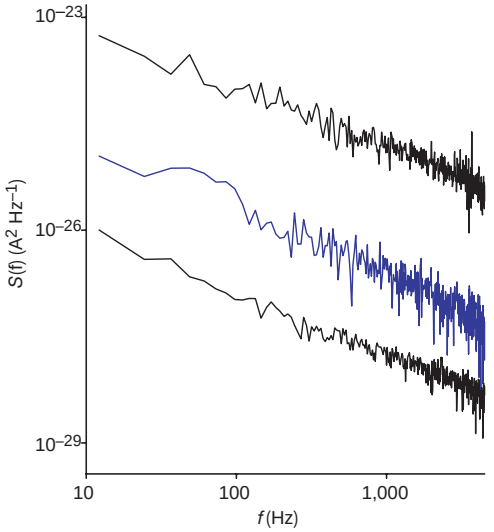

Figure 3 Power spectras of whole-cell (top and middle traces) and single-channel (bottom trace) currents. Spectra were calculated from recordings in solution A (middle trace) or solution A plus 1,000 mM choline$^+$Cl$^-$ (top and bottom traces). These profiles are roughly parallel, indicating that the single-channel type seen with on-cell patch clamp can fully account for the whole-cell currents. The $1/f$ profiles reflect the complexity of single-channel bursting.

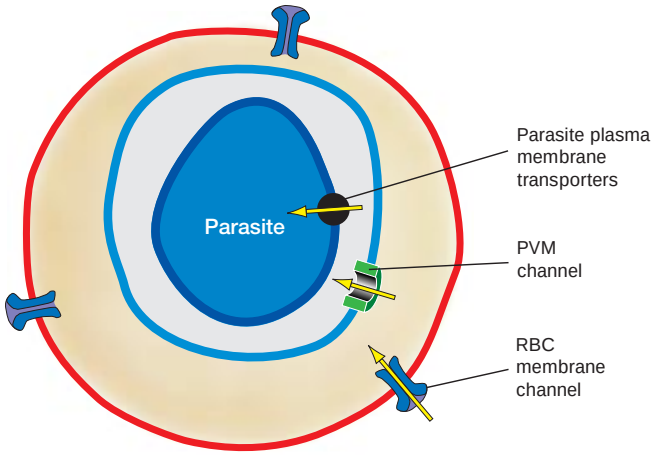

Figure 4 Sequential route of nutrient acquisition. In addition to entry through endogenous RBC carriers (not shown), key nutrients in serum are acquired by sequential passage through the voltage-dependent anion channel on the RBC membrane, the non-selective PVM channel and carriers on the parasite plasma membrane. The parasitophorous duct, if present, would produce continuity between the PVM and RBC membranes. Although not shown here, the PVM has extensive invaginations (called the tubulovesicular network[27]) that probably increase its surface area for nutrient uptake by the PVM channel.

Methods

Whole-cell conductances

We took human RBCs from a healthy volunteer, washed them in solution A (in mM: 115 NaCl, 10 $MgCl_2$, 5 $CaCl_2$, 20 Na-HEPES, pH 7.4), and allowed them to settle before patch clamp. Pipettes were pulled from Corning 7056 glass to tip diameters $\leq 0.5\ \mu m$ (1–5 MΩ), heat-polished, filled with filtered pipette solutions and used immediately. For whole-cell recordings, we obtained patch rupture by applying electrical pulses until a capacitive transient developed. Although the whole-cell configuration is usually achieved on other cells by suction applied to the pipette[24], this often damaged the small RBC. *Plasmodium falciparum* trophozoites, grown in the same RBCs[25], were voltage clamped by the same methods. Whole-cell recordings were filtered at 10 kHz (8 pole Bessel filter). Data for current–voltage profiles represent the current averaged over 20–50 ms. Furosemide had no effect on uninfected RBC currents (data not shown).

Anion selectivity

We determined Na^+ versus Cl^- selectivity with a uncharged solute as the primary osmolyte in the pipette (solution B: (in mM) 230 sorbitol, 20 Na-HEPES, 10 $MgCl_2$, 0.5 EGTA, pH 7.4) to quantitate relative influx of cations and anions. Similar results were obtained with sucrose as the primary osmolyte in the pipette (not shown).

Selectivity of anions was determined under biionic conditions with a bath solution of (in mM) 500 NaCl, 10 $MgCl_2$, 5 $CaCl_2$, 20 Na-HEPES, pH 7.4, and pipette solutions of (in mM) 500 Na^+ salt of the test anion (436 for lactate$^-$), 10 $MgCl_2$, 20 Na-HEPES, pH 7.4. P/P_{Cl} were then calculated with the Goldman equation[26] using the mean E_{rev}.

Channel characterization

We carried out single-channel measurements in hypertonic saline to increase conductance through this channel and to reduce pipette noise by reducing access resistance, both of which improved our signal-to-noise ratio. Single-channel recordings were filtered at 6 kHz and digitized at 100 kHz.

We carried out spectral analysis of whole-cell and single-channel recordings on 1-s current sweeps recorded at V_m of +40 mV after filtering at 15 kHz (8 pole Butterworth filter). For each trace, the power spectrum of non-channel noise (for example, from equipment), determined at $V_m = 0$, was subtracted. The power spectrum of a single burst of channel activity was adequately described by a Lorentzian with a characteristic time of 0.5 ms (not shown).

Received 30 May; accepted 2 July 2000.

1. Kirk K., Horner, H. A., Elford, B. C., Ellory, J. C. & Newbold, C. I. Transport of diverse substrates into malaria-infected erythrocytes via a pathway showing functional characteristics of a chloride channel. *J. Biol. Chem.* **269,** 3339–3347 (1994).
2. Ginsburg, H., Kutner, S., Krugliak, M. & Cabantchik, Z. I. Characterization of permeation pathways appearing in the host membrane of *Plasmodium falciparum* infected red blood cells. *Mol. Biochem. Parasitol.* **14,** 313–322 (1985).
3. Upston, J. M. & Gero, A. M. Parasite-induced permeation of nucleosides in *Plasmodium falciparum* malaria. *Biochim. Biophys. Acta* **1236,** 249–258 (1995).
4. Cabantchik, Z. I. Properties of permeation pathways induced in the human red cell membrane by malaria parasites. *Blood Cells* **16,** 421–432 (1990).
5. Staines, H. M., Rae, C. & Kirk, K. Increased permeability of the malaria-infected erythrocyte to organic cations. *Biochim. Biophys. Acta* **1463,** 88–98 (2000).
6. Burns, E. R. & Pollack, S. *P. falciparum* infected erythrocytes are capable of endocytosis. *In Vitro Cell Dev. Biol.* **24,** 481–486 (1988).
7. Pouvelle, B. *et al.* Direct access to serum macromolecules by intraerythrocytic malaria parasites. *Nature* **353,** 73–75 (1991).
8. Hunter, M. J. Human erythrocyte anion permeabilities measured under conditions of net charge transfer. *J. Physiol. (Lond.)* **268,** 35–49 (1977).
9. Kirk, K. & Horner, H. A. Novel anion dependence of induced cation transport in malaria-infected erythrocytes. *J. Biol. Chem.* **270,** 24270–24275 (1995).
10. Kirk, K., Horner, H. A., Spillett, D. J. & Elford, B. C. Glibenclamide and meglitinide block the transport of low molecular weight solutes into malaria-infected erythrocytes. *FEBS Lett.* **323,** 123–128 (1993).
11. Kutner, S., Breuer, W. V., Ginsburg, H. & Cabantchik, Z. I. On the mode of action of phlorizin as an antimalarial agent in *in vitro* cultures of Plasmodium falciparum. *Biochem. Pharmacol.* **36,** 123–129 (1987).
12. Breuer, W. V., Kutner, S., Sylphen, J., Ginsburg, H. & Cabantchik, Z. I. Covalent modification of the permeability pathways induced in the human erythrocyte membrane by the malarial parasite *Plasmodium falciparum*. *J. Cell. Physiol.* **133,** 55–63 (1987).
13. Wright, E. M. & Diamond, J. M. Anion selectivity in biological systems. *Physiol. Rev.* **57,** 109–156 (1977).
14. Desai, S. A., Krogstad, D. J. & McCleskey, E. W. A nutrient-permeable channel on the intraerythrocytic malaria parasite. *Nature* **362,** 643–646 (1993).
15. Ginsburg, H. & Stein, W. D. Biophysical analysis of novel transport pathways induced in red blood cell membranes. *J. Membr. Biol.* **96,** 1–10 (1987).
16. Sauve, R. & Szabo, G. Interpretation of 1/f fluctuations in ion conducting membranes. *J. Theor. Biol.* **113,** 501–516 (1985).
17. Divo, A. A., Geary, T. G., Davis, N. L. & Jensen, J. B. Nutritional requirements of *Plasmodium falciparum* in culture. I. Exogenously supplied dialyzable components necessary for continuous growth. *J. Protozool.* **32,** 59–64 (1985).

© 2000 Macmillan Magazines Ltd

18. Kirk, K., Horner, H. A. & Kirk, J. Glucose uptake in *Plasmodium falciparum*-infected erythrocytes is an equilibrative not an active process. *Mol. Biochem. Parasitol.* **25,** 195–205 (1996).
19. Carter, N. S. *et al.* Isolation and functional characterization of the PfNT1 nucleoside transporter gene from *Plasmodium falciparum*. *J. Biol. Chem.* **275,** 10683–10691 (2000).
20. Hibbs, A. R., Stenzel, D. J. & Saul, A. Macromolecular transport in malaria–does the duct exist? *Eur. J. Cell Biol.* **72,** 182–188 (1997).
21. Crandall, I. & Sherman, I. W. *Plasmodium falciparum* (human malaria)-induced modifications in human erythrocyte band 3 protein. *Parasitology* **102,** 335–340 (1991).
22. Bull, P. C. *et al.* Parasite antigens on the infected red cell surface are targets for naturally acquired immunity to malaria. *Nature Med.* **4,** 358–360 (1998).
23. Elford, B. C., Cowan, G. M. & Ferguson, D. J. Parasite-regulated membrane transport processes and metabolic control in malaria-infected erythrocytes. *Biochem. J.* **308,** 361–374 (1995).
24. Hamill, O. P., Marty, A., Neher, E., Sakmann, B. & Sigworth, F. J. Improved patch-clamp techniques for high-resolution current recording from cells and cell-free membrane patches. *Pflugers Arch.* **391,** 85–100 (1981).
25. Trager, W. & Jensen, J. B. Human malaria parasites in continuous culture. *Science* **193,** 673–675 (1976).
26. Goldman, D. E. Potential, impedance, and rectification in membranes. *J. Gen. Physiol.* **27,** 36–60 (1943).
27. Lauer, S. A., Rathod, P. K., Ghori, N. & Haldar, K. A membrane network for nutrient import in red cells infected with the malaria parasite. *Science* **276,** 1122–1125 (1997).

Acknowledgements

We thank L. Miller for steady help and advice, and S. Brazer, F. Cohen, A. Sher and T. Wellems for reviewing the manuscript.

Correspondence and requests for materials should be addressed to S.A.D. (e-mail sdesai@niaid.nih.gov).

Effects of oncogenic mutations in *Smoothened* and *Patched* can be reversed by cyclopamine

Jussi Taipale*, James K. Chen*, Michael K. Cooper†*, Baolin Wang*, Randall K. Mann*, Ljiljana Milenkovic‡, Matthew P. Scott‡ & Philip A. Beachy*

** Department of Molecular Biology and Genetics, and † Department of Neurology, Howard Hughes Medical Institute, The Johns Hopkins University School of Medicine, Baltimore, Maryland 21205, USA*
‡ Departments of Developmental Biology and Genetics, Howard Hughes Medical Institute, Stanford University School of Medicine, Stanford, California 94305-5427, USA

Basal cell carcinoma, medulloblastoma, rhabdomyosarcoma and other human tumours are associated with mutations that activate the proto-oncogene *Smoothened* (*SMO*) or that inactivate the tumour suppressor *Patched* (*PTCH*). Smoothened and Patched mediate the cellular response to the Hedgehog (Hh) secreted protein signal, and oncogenic mutations affecting these proteins cause excess activity of the Hh response pathway[1,2]. Here we show that the plant-derived teratogen cyclopamine, which inhibits the Hh response[3,4], is a potential 'mechanism-based' therapeutic agent for treatment of these tumours. We show that cyclopamine or synthetic derivatives with improved potency block activation of the Hh response pathway and abnormal cell growth associated with both types of oncogenic mutation. Our results also indicate that cyclopamine may act by influencing the balance between active and inactive forms of Smoothened.

Whereas embryonic loss of Sonic hedgehog (Shh) signalling can result in cyclopia and other developmental defects[5], inappropriate activation of the Shh response pathway is associated with several types of human tumour[6–13]. Current approaches to treatment of such neoplastic disorders are limited by the cytotoxic effects of therapeutic agents on proliferating tissues. Alternative 'mechanism-based' approaches specifically targeting abnormally active signalling pathways in defined types of cancer[14] might avoid such toxicity, particularly if the pathways in question functioned primarily in embryonic development and were not required for survival in adults. Cyclopamine, a plant steroidal alkaloid, induces cyclopia in vertebrate embryos[15] and has been shown to act by inhibiting the cellular response to the Shh signal[3,4]. To evaluate the therapeutic potential of cyclopamine for the treatment of Hh-pathway-associated disorders we investigated the mechanism by which cyclopamine acts.

Cellular responses to the Hh signal are controlled by two transmembrane proteins, Smo and Ptch, which are predicted to have seven and twelve transmembrane spans, respectively. Genetic and biochemical evidence indicates that Ptch suppresses the activity of Smo, and that binding of Hh to Ptch relieves this suppression[1,2], allowing activation of downstream targets through the Ci/Gli family of transcriptional effectors[16–19]. As our previously described Hh signalling assay used *Drosophila melanogaster* cultured cells and was not sensitive to cyclopamine (ref. 18 and data not shown), we screened several vertebrate cell lines for a sensitive transcriptional response to palmitoyl- and cholesteryl-modified ShhN polypeptide ($ShhN_p$)[20] (Fig. 1a) using a Gli-dependent luciferase reporter[21]. Among several responsive fibroblast cell lines, NIH-3T3 mouse embryonic fibroblasts, which respond with a 20–150-fold induction of luciferase activity (Fig. 1b), were selected for all further studies except those requiring particular genetic backgrounds. Treatment of the cells with cyclopamine completely abolished the response to $ShhN_p$ (Fig. 1c). To confirm the validity of this assay, we analysed the

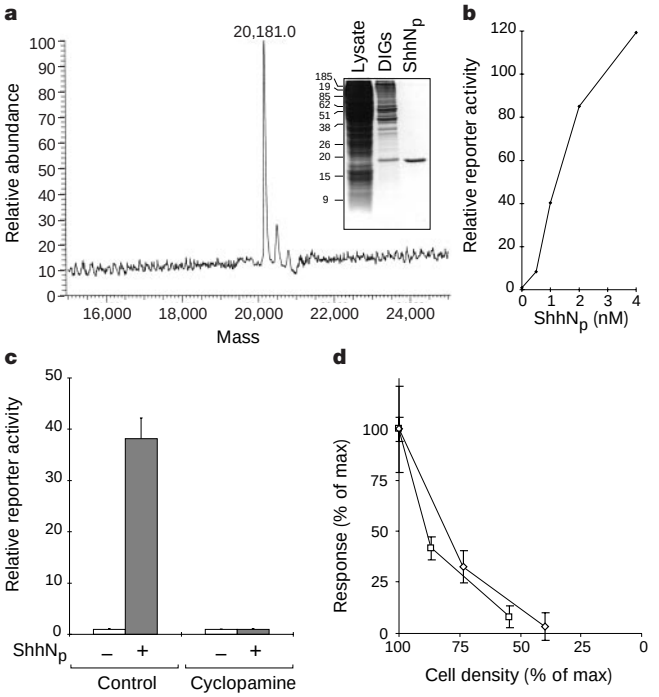

Figure 1 NIH-3T3 fibroblasts respond to $ShhN_p$ and are sensitive to cyclopamine. **a**, Sonic hedgehog signalling domain was purified by isolating detergent-insoluble glycolipid complexes (DIGs) from 293 cells expressing full-length Shh[3], followed by immunoaffinity chromatography. The purified species corresponds to palmitoyl- and cholesteryl-modified ShhN polypeptide ($ShhN_p$) from mass spectrometry analysis. Inset, SDS–polyacrylamide gel electrophoresis analysis of lysate, DIGs and purified $ShhN_p$. The responsiveness of NIH-3T3 cells to Shh (**b**) and cyclopamine (**c**) was analysed by transfection with Gli-luc reporter and Renilla luciferase control followed by treatment with $ShhN_p$ (4 nM or as indicated) and/or cyclopamine (5 μM) for 2 d. Luciferase activities normalized relative to control. For time response, see Supplementary Information. **d**, The effect of cell density on Shh pathway activity was analysed by plating cultures of stable Shh reporter lines Shh-LIGHT (squares) or SmoA1-LIGHT (diamonds) cells in quadruplicate to 96-well plates in a series of twofold dilutions. The Shh-LIGHT cells were treated with 4 nM $ShhN_p$, and Gli-luc reporter activity (relative to equally dense Shh-LIGHT control culture) and relative cell density (% of maximum Renilla activity) were assayed after 24 h. Error bars, 1 s.d.

© 2000 Macmillan Magazines Ltd